POD-ISAT : An Efficient Reduced-order Modeling Method for the representation of Parametrized Finite Element solutions. Application to Aircraft Air Control Systems

Dung Bui, Mohamed Hamdaoui, Florian de Vuyst

INTERNATIONAL JOURNAL FOR NUMERICAL METHODS IN ENGINEERING
Int. J. Numer. Meth. Engng 2010; **00**:1–21
Published online in Wiley InterScience (www.interscience.wiley.com). DOI: 10.1002/nme

POD-ISAT : A New and Efficient Reduced-order Modeling Method for the representation of Parametrized Finite Element solutions. Application to Aircraft Air Control Systems

D. BUI[1,2,*], M. HAMDAOUI[1], F. De VUYST[2]

[1] *Laboratoire de Mathématiques Appliquée aux Systèmes (MAS), École Centrale de Paris, Grande voie des vignes, 92295 Châtenay-Malabry, France*

[2] *Centre de Mathématiques et de Leurs Applications (CMLA), École Normale Supérieure de Cachan, 61, avenue du Président Wilson 94235 Cachan cedex, France*

SUMMARY

A combination of Proper Orthogonal Decomposition (POD) and In Situ Adaptive Tabulation (ISAT) is proposed for the representation of parameter-dependent solutions of coupled partial differential equations (PDE). The accuracy of the method is easily controlled by open parameters that can be adjusted according to the users needs. The method is tested on a coupled fluid-thermal problem: the design of a simplified aircraft air control system. It is successfully compared to the standard POD: while the POD is inaccurate in certain areas of the design parameters space, the POD-ISAT method achieves accuracy thanks to residual based on trust regions. The presented POD-ISAT approach provides flexibility, robustness and tunable accuracy to represent solutions of parametrized PDEs. Copyright © 2010 John Wiley & Sons, Ltd.

Received . . .

KEY WORDS: Multiphysics Problems, Reduced-Order Modeling (ROM), nonintrusive, In-Situ-Adaptive-Tabulation (ISAT), Proper Orthogonal Decomposition (POD), Aircraft air control system.

1. INTRODUCTION

Computational tools are today a success factor in Engineering Design. Finite Elements or Finite Volumes codes become very efficient in the evaluation of criteria at given design points. However, the 'full' exploration of the design space is still a difficult task because of the curse of dimensionality and the weak computing performance available for such applications. Alternative solutions are the use of meta-models or low-order optimal bases that show both accuracy and computational efficiency for particular classes of problems (elliptic problems). Proper Orthogonal Decomposition (POD) [1], Goal-oriented approaches [2, 3], Reduced Basis Method (RBM) [4, 5], LATIN methodology [6] or Proper Generalized Decompositions (PGD) [7], Hyperreduction method [8] are among the most known computational approaches for dimensionality reduction of PDE solutions. But there are still big issues such as the case of hyperbolic problems, convection-dominated problems, strongly coupled multi-physics problems, high-dimensional design spaces, etc.
The present paper deals with the design of reduced order modelling technique that the foreseen application is a simplified aircraft air control system depending on inflow and exterior conditions.

*Correspondence to: Dung Bui, Laboratoire de Mathématiques Appliquée aux Système, École Centrale de Paris, Grande voie des vignes, 92295 Châtenay-Malabry, France.
†E-mail: dung.bui@ecp.fr

Navier-Stokes equations are coupled with a thermal equation by means of a buoyancy force (Boussinesq approximation). In this work, an innovating approach called POD-ISAT is presented. It combines Proper Orthogonal Decomposition for the representation of the spatial fields and In Situ Adaptive Tabulation (ISAT) for the local representation of the solution in the design space. This leads to a set of local reduced-order models whose fidelity is controlled by means of trust regions (TR). In Pope's ISAT model [9, 10], ellipsoids of accuracy (EOA) are used and adapted during the learning process of the table. Here we rather use a threshold criterion on a residual. The whole algorithm is detailed in the paper and numerical results show the efficiency of the approach.
The remaining section of the paper is organized as follows. In section 2, aircraft environment control system is discussed. In section 3, we introduce a real test case on the design of aircraft air control system. Then we present in section 4 the methodology of reduced order modelling (ROM) in the literature. In section 5, a new ROM method so called POD-ISAT is presented. Numerical experiments are presented in section 6. Some interesting results of residual depending on the design parameters and on the number of used POD basis functions are analysed. The accurate and efficiency (speed-up) of POD-ISAT are proved. We compare also the accurate of this method and the POD non intrusive model. Concluding remarks and perspectives are discussed in the last section.

2. AIR AIRCRAFT CABIN COMFORT ANALYSIS

Aircraft cabin comfort is today a key factor in aircraft design. The airline industry suppliers of aircraft and interior furnishings have made great efforts to satisfy passengers needs as cabin comfort plays an important role in airline ticket sales: improving aircraft comfort attracts more passengers. Therefore, it is essential to pay attention to the quality of the air of the cabin to ensure that it is comfortable for all passengers. More and more passengers including those with impaired health or those who are sensitive to cabin environmental conditions plan their travel. They request a safe and comfortable cabin environment because they may encounter a combination of environmental factors including low or high temperature, low humidity, low air pressure, and sometimes exposure to air contaminants such as carbon monoxide, ozone, various organic compounds [11]. It has been reported that international air travel include potential risks associated with airborne disease transmission [12, 13]. On a flight from Hong Kong to Beijing 22 passengers out of 120 were infected with the Severe Acute Respiratory Syndrome (SARS) [14].
Furthermore, the external environment of the aircraft changes between the different flight phases (taxiing, take-off, cruise, and descent). The outside temperature varies from $-55°C$ to over $50°C$, the ambient pressure varies from about 10.1 kPa (at altitude of $11\,kms$) to 101 kPa (at sea level) and the water content changes from virtually dry to greater than saturation. To transport people in those varying external conditions, aircrafts are equipped with environmental control systems (ECSs) that provide suitable indoor environments. The ECS consists in a complex set of air treatment and heat exchange systems, sensors and controllers and is part of the aircraft's electric, pneumatic and hydraulic systems. It's behaviour significantly depends on the airflow and heat exchange in the aircraft cabin.
Recently, many scientists focused their attention on improving the ECS of future aircrafts to provide a comfortable cabin at minimal consumed power. Zhang et al. [15, 16] proposed a novel air distribution system adding an under-floor air inflow system and a personalized air inflow system in front of passenger head. Their results showed that the novel ECS provides the best air quality without draft risk. Vankan et al. [17] investigated and evaluated efficient methodologies for approximate representation of steady-state system behaviour in aircraft cabin, applied to a design case of a power optimized aircraft. In these studies, the authors assumed that the phase of flight mission and the related on-board services and activated systems mainly contribute to the power consumption providing the air-conditioning in the cabin.
An important element of passenger satisfaction is thermal conform. The major factors involved in thermal comfort are the air temperature, relative humidity, air refreshment rate, heat radiation and clothing. The research about this problem is initiated by Franger [18], and then improved by Kok et al. [19] in the framework of the European project FACE (Friendly Aircraft Cabin Environment).

DOI: 10.1002/nme

In these works, the numerical simulation of the three major phenomena that play a significant role in thermal comfort were considered: the human response to its thermal environment which is also known as thermal regulation, the actual movement of air and heat inside aircraft cabins due to natural and/or forced convection, and heat transfer due to radiation. For the first one, the thermal regulation model of Tanabe [20] which simulate the thermal exchange in sixteen different human body segments with environment air is used. The second one used a CFD model based on a weakly compressible Reynolds-averaged Navier-Stokes (RANS) formulation. The third one employed the surface-to-surface radiation model consisting in an integral equation, which relates radiation flux leaving the enclosing surface to the temperature distribution of this surface. The thermal regulation and radiation models are coupled with the flow model, but not directly with each other. These two coupled models are solved by iterative schemes. Note that a CFD model is a system of non-linear equations which can be very time consuming to solve. Moreover, the air flow in cabin depends not only on the human body thermal and heat radiation but on the air supplied by ECS. Ideally, one would like to explore the parameter design space, in order to find or choose attractive designs, or to optimize according to some criteria and constraints. In this case we face a high-dimensional problem where each design point requires a CFD solution. Therefore, a reduced order modelling method for parametrized CFD models is required.
A CFD model solves numerically a set of partial differential equations (PDEs) for the conservation of mass, momentum, energy, chemical-species concentrations, and turbulence quantities. The solutions are the field of air velocity, air temperature, the concentrations of water vapour and contaminants, and turbulence parameters in an aircraft cabin. These solutions depend on the boundary and initial conditions. Liu et al. [21] summarized all the numerical studies on the flow in an aircraft cabin published in the past two decades. The most used CFD models are RANS models and Large Eddy Simulation (LES) models.
Generally, aircraft cabin airflow depends on many parameters which are almost boundary conditions of CFD models:

- the heat source of passenger body, of galley switched on to prepare hot meals, and of electric device;
- external environment: temperature and pressure;
- inflow temperature;
- inflow velocity;
- position and orientation of inflow air;
- fuselage thermal conductivity.

To build a ROM we propose in the next section a simple CFD model coupling Navier-Stokes equation and thermal diffusion equation that takes in to account several parameters.

3. MATHEMATICAL SETTING

We are interested in the modelling of stationary air circulation and heating conditions in an aircraft cabin. For the sake of simplicity, the flow is supposed two-dimensional and the domain of interest is the cross-section of the fuselage (see figure 1). The air is seen as an incompressible fluid but we take into account buoyancy Archimedes forces due to air dilatability by heating. So the stationary Navier-Stokes equations with the Boussinesq approximation are considered. At the right hand side of the Navier-Stokes momentum equation (2) appears a buoyancy term depending on the gravity $\boldsymbol{g}$ and the temperature deviation $(T - T_0)$ from the nominal temperature T_0. The Navier-Stokes equations are coupled, through this buoyancy term, with a thermal equation that governs the evolution of the temperature of the fluid (equations (1)-(3)). The coefficient κ is the thermal diffusivity of the air.

$$\nabla \cdot \boldsymbol{u} = 0 \quad \text{in } \Omega, \tag{1}$$

$$\boldsymbol{u} \cdot \nabla \boldsymbol{u} - \nu \Delta \boldsymbol{u} + \nabla p = \boldsymbol{g}\ (1 - \alpha(T - T_0)) \quad \text{in } \Omega, \tag{2}$$

$$\boldsymbol{u} \cdot \nabla T - \nabla \cdot (\kappa \nabla T) = 0 \text{ in } \Omega, \tag{3}$$

DOI: 10.1002/nme

In realistic conditions, the reference length L is 1 m, the characteristic speed U is 1 m/s and the kinematic viscosity of the air at 300 K is $1.57\,10^{-5}\ m^2/s$ so that the Reynolds number is equal to

$$Re = \frac{LU}{\nu} \approx 6.37\,10^4.$$

For this Reynolds number the flow regime is turbulent, but, for the sake of simplicity, we do not take into account any turbulence model here. Moreover the thermal diffusivity of air at 300 K and 1 atm is $2.22\,10^{-5}\ m^2/s$, thus the Péclet number is

$$Pe = \frac{LU}{\kappa} \approx 4.52\,10^4.$$

meaning that the thermal convection-diffusion problem dominated by convection. Furthermore, the air thermal expansion coefficient α is $3.43\,10^{-3}K^{-1}$ and the maximal temperature variation ΔT is 10 K thus the Archimedes number Ar is

$$Ar = \frac{g\alpha\Delta T L^3}{\nu^2 Re} \approx 0.2,$$

which means that the flow is dominated by forced convection.

Let us now consider the boundary conditions. The cabin boundary is denoted Γ. It is divided into

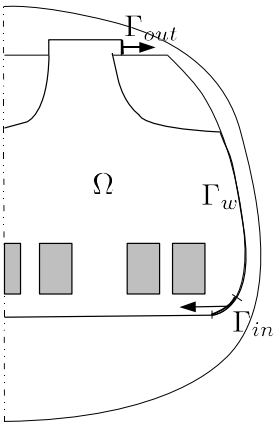

Figure 1. Spatial geometry and domain boundaries (half domain with symmetry axis)

three parts: the inflow boundary Γ_{in}, the outflow Γ_{out} and the wall boundary Γ_w. For the fluid, no slip boundary conditions is used on Γ_w, velocity is imposed at the inflow and constant pressure is given at the outflow:

$$\boldsymbol{u} = 0 \text{ on } \Gamma_w,\ \boldsymbol{u} = \boldsymbol{u}_{in} \text{ on } \Gamma_{in} \text{ and } p = 0 \text{ on } \Gamma_{out}. \tag{4}$$

For thermal boundary conditions, we used Dirichlet boundary conditions on Γ_{in} with imposed inflow temperature T_{in}. The heat loss at the walls is expressed by inhomogeneous Fourier boundary conditions. The boundary heat flux may depend on the difference between the wall temperature and the exterior temperature. Finally, homogeneous Neumann boundary conditions are written at the outflow:

$$T = T_{in} \text{ on } \Gamma_{in},\ \frac{\partial T}{\partial n} = 0 \text{ on } \Gamma_{out},\ \kappa\frac{\partial T}{\partial n} = \Phi(T - T_{ext}) \text{ on } \Gamma_w. \tag{5}$$

Possibly, if interior boundaries are defined (like seats for example), then homogeneous Neumann boundary conditions are imposed. The whole system is non-linear and the dominating phenomenon is the convection (because of the large Reynolds and Péclet numbers). It is assumed that the domain boundaries are Lipschitz continuous, $\boldsymbol{u}_{in}, T_{in} \in H^{1/2}(\Gamma_{in})$, $\Phi \in \mathcal{C}^\infty$, so that $(\boldsymbol{u}, p, T)$ are searched

DOI: 10.1002/nme

in $U_{u_{in}} \times L^2(\Omega) \times X_{T_{in}}$, where

$$U_w = \left\{ \boldsymbol{v} \in [H^1(\Omega)]^2,\ \boldsymbol{v} = 0 \text{ on } \Gamma_w,\ \boldsymbol{v} = \boldsymbol{w} \text{ on } \Gamma_{in} \right\},$$

$$X_w = \left\{ \tau \in H^1(\Omega),\ \tau = w \text{ on } \Gamma_{in} \right\}.$$

According to some approximate candidates $\tilde{\boldsymbol{u}} \in U_{u_{in}}$, $\tilde{p} \in L^2(\Omega)$ and $\tilde{T} \in X_{T_{in}}$, one can define a residual functional relative to the test functions $\boldsymbol{v} \in U_0$, $q \in L^2(\Omega)$ and $\tau \in X_0$:

$$\begin{aligned} R(\tilde{\boldsymbol{u}}, \tilde{p}, \tilde{T}, \boldsymbol{v}, q, \tau) &= \int_\Omega (\tilde{\boldsymbol{u}} \cdot \nabla \tilde{\boldsymbol{u}}) \cdot \boldsymbol{v}\, dx + \int_{\Gamma_{out}} \frac{\partial \tilde{\boldsymbol{u}}}{\partial \boldsymbol{n}} \cdot \boldsymbol{v}\, d\sigma - \int_\Omega \tilde{p}\, \nabla \cdot \boldsymbol{v}\, dx \\ &- \int_\Omega (1 - \alpha(\tilde{T} - T_0))\, \boldsymbol{g} \cdot \boldsymbol{v}\, dx + \int_\Omega \nabla \cdot \tilde{\boldsymbol{u}}\, q\, dx + \int_\Omega (\tilde{\boldsymbol{u}} \cdot \nabla \tilde{T}) \tau\, dx \\ &- \int_\Omega \kappa\, \nabla \tilde{T} \cdot \nabla \tau\, dx - \int_{\Gamma_w} \Phi\, (\tilde{T} - T_{ext}) \tau\, d\sigma \quad \forall (\boldsymbol{v}, q, \tau) \in U_0 \times L^2(\Omega) \times X_0. \end{aligned} \tag{6}$$

Remember that the problem depends on the parameters. For our reference problem, we will assume that the parameters act on the inflow temperature T_{in} and the fuselage's thermal conductivity κ_f. Using dimensionless parameters $\theta_i \in [-1, 1]$, $i = 1, \ldots, p$, we are looking for the family of fluid-thermal solutions $\left(\boldsymbol{u}^\theta = \boldsymbol{u}(\theta, .),\, T^\theta = T(\theta, .)\right)_{\theta \in [-1,1]^p}$. In this paper, we are interested in building ROMs for the temperature field $T(\theta, x)$. According to some approximate candidates $\tilde{\boldsymbol{u}} \in U_{u_{in}}$ and $\tilde{T} \in X_{T_{in}}$ the following residual is used:

$$\forall \tau \in X_0, \quad R(\tilde{T}, \tau, \tilde{\boldsymbol{u}}) = \int_\Omega (\tilde{\boldsymbol{u}} \cdot \nabla \tilde{T}) \tau\, dx - \int_\Omega \kappa\, \nabla \tilde{T} \cdot \nabla \tau\, dx - \int_{\Gamma_w} \Phi\, (\tilde{T} - T_{ext}) \tau\, d\sigma \tag{7}$$

The use of the residual in (7) is supported by the low value of the Ar number that indicates that the heat transfer is dominated by convection and that the Boussinesq term that appears in (2) can be neglected. The function $\Phi \in \mathcal{C}^\infty$ that defines the heat flux at the fuselage is given by:

$$\forall x \in \mathbb{R}, \quad \Phi(x) = \frac{\kappa_f}{e} x, \tag{8}$$

with e the fuselage thickness and κ_f the fuselage thermal conductivity.

4. ROM METHODOLOGY: GENERAL ASPECTS AND RELATED WORKS

A Reduced Order Modelling (ROM) approach for partial differential equations consists in a low-order representation of the solution by help of a low-order optimal basis and possibly an adaptivity and enrichment process. Considering for example the parametrized temperature field $T^\theta = T(., \theta)$, reduced-order models are searched in the form

$$T^\theta(x) = T^{lift,\theta}(x) + \sum_{k=1}^{K} a_k(\theta)\, \boldsymbol{\Psi}^k(x). \tag{9}$$

The function $T^{lift,\theta}$ is a lifting function aimed at satisfying some boundary conditions (especially Dirichlet BC), possibly depending on θ but quite easy to compute (for example the solution of a linear Stokes Problem). The family $(\boldsymbol{\Psi}^k)_{k=1,\ldots,K}$ is the 'optimal' basis. The truncation rank K is expected to be rather small, let us say 10. The expansion coefficients $a_k(\theta)$ are functions depending on the vector parameter $\theta \in [-1, 1]^p$. In a ROM methodology, there are two main steps: the design of the basis functions $\boldsymbol{\Psi}^k$ and the learning process of the $a_k(\theta)$. In the POD snapshot approach [1, 22], some snapshot fields $(T^i)_{i=1,\ldots,N}$ are computed according to a Design of Computer Experiment (DoCE). Then, the POD basis spawns the best linear subspace able to represent the snapshot

DOI: 10.1002/nme

solutions:

$$\min_{\substack{(\boldsymbol{\Psi}^1,\ldots,\boldsymbol{\Psi}^K)\\(\boldsymbol{\Psi}^k,\boldsymbol{\Psi}^\ell)=\delta_{k\ell},\ 1\leq k\leq \ell\leq N}} \frac{1}{2}\sum_{i=1}^{N}\left\| T^i - T^{lift,\theta^i} - \sum_{k=1}^{K}(T^i - T^{lift,\theta^i},\boldsymbol{\Psi}^k)\,\boldsymbol{\Psi}^k \right\|^2, \tag{10}$$

which is equivalent to solve the problem of maximum correlation:

$$\max_{\substack{(\boldsymbol{\Psi}^1,\ldots,\boldsymbol{\Psi}^K)\\(\boldsymbol{\Psi}^k,\boldsymbol{\Psi}^\ell)=\delta_{k\ell},\ 1\leq k\leq \ell\leq N}} \frac{1}{2}\sum_{i=1}^{N}\sum_{k=1}^{K}(T^i - T^{lift,\theta^i},\boldsymbol{\Psi}^k)^2. \tag{11}$$

In the POD methodology, the $(\boldsymbol{\Psi}^k)$ are said to be an empirical basis because of the empirical choice of the snapshot set (see [23] for a recent analysis on the optimal location of the snapshots). Reduced Basis Methods or RBM [4, 5] are more rigorous approaches where the basis is enriched during an iterative learning process. At a given iteration (k) involving k modes, a $(k+1)th$ mode Ψ^{k+1} is searched as a best corrector direction corresponding to the the worst case location in the parameter domain. This is a kind of 'min-max' algorithm. RBM involves easy-to-compute accuracy estimators; we refer to the literature ([24, 25, 26]) for this issue. Because of the iterative enrichment process, RBM belongs to the family of greedy algorithms. Let us emphasize that the RBM analysis framework is mainly restricted to elliptic problems. Another and recent approach which knowns an increasing interest is the Proper Generalized Decomposition or PGD, introduced by Ladevze in the context of the LATIN method (LArge Time INcrement method) for reducing computational costs. Then it is extended and used in many fields of applications ([7, 27, 28, 29, 30, 31]). PGD is also a greedy algorithm where the variables are separated. From a level-k model $\tilde{T}^{(k)}(\theta,.)$, a higher-fidelity model $\tilde{T}^{(k+1)}(\theta,.)$ is searched in the form

$$\tilde{T}^{(k+1)}(\theta,.) = \tilde{T}^{(k)}(\theta,.) + a_1^{(k+1)}(\theta_1)\,a_2^{(k+1)}(\theta_2)\ldots a_p^{(k+1)}(\theta_p)\,\boldsymbol{\Psi}^{(k+1)}(x), \tag{12}$$

where the one-dimensional functions $a_1^{(k+1)}(\theta_1)$, $a_2^{(k+1)}(\theta_2)$ $\ldots$ $a_p^{(k+1)}(\theta_p)$ and the spatial model $\boldsymbol{\Psi}^{(k+1)}(x)$ are searched in an optimal way, for example by a variational principle and a Galerkin projection, see references [7, 32] for more details. Although very promising, PDG still needs investigation especially for parameter problems. It is unclear from the numerical analysis point of view what is the truncation rank K for a given error criterion. Moreover, PGD for the moment is an intrusive approach, what can be a shortcoming in a practical industrial context. PGD also needs more developments in the case of coupled problems. Our paper aims at developing a non-intrusive approach based on FE or FV code without modification to the reference code. So we refer to a formalism of non-intrusive physics-based meta-modelling proposed by P.B Nair ([33]) which will be used in this work. This meta-modelling technique was then extended by ([34]) using POD method for spatial approximation within RBF interpolation of POD coefficients. They proposed two variants of ROM algorithms. The first one is based on both spatial and parameter space POD decompositions. The second one uses only POD decompositions in spatial space and models the coefficients of the decomposition as general functions of the parameter vector θ. The principle is to determine in off-line stage the coefficients $a_k(\theta)$ in (9) by minimizing a function based on the residual returned by the fine solver. We assume that this computation is far less expressive than the fine FE computation. Indeed, the rank K is expected to be small, typically in the range $[4, 10]$, whereas the FE dimension is of order $10^5 - 10^6$ for a two-dimensional problem, and $10^6 - 10^7$ for a three-dimensional one. A classical approach to determine the POD coefficients $a_k(\theta)$ is to use a design of computer experiments (DoCE) to sample the parameter space, then to interpolate the obtained data set using meta-modelling methodology (RBF for instance). Note that for a parallel computer architecture, all these sample computations can be done in parallel. For some problems or applications, the spatial structure of the solution may strongly depend on the parameters meaning the spatial components strongly change within the parameter space. To get a global model with all the spatial structure, this would involve a higher rank truncation K (say between 20 and 90 as

DOI: 10.1002/nme

illustration) thus reducing the ROM efficiency. In general case, there are large zones of parameter space where the solution shape does not change strongly. Our idea is to build a local adaptive POD ROM for zones centred on a sample in the parameter space. In each zone, we need only some POD modes to capture enough information. We suggest an In-Situ Adaptive Tabulation (ISAT) approach [10] combined with the POD for low-order spatial representation. The so called POD-ISAT algorithm is an easy-to-implement non-intrusive approach that can be used in an industrial context.

5. THE POD-ISAT ALGORITHM

The determination of POD modes by the method of snapshots [1] relies on the prior computation of some accurate finite element solutions. A very popular physics-based meta-modelling technique, namely the POD-Galerkin approach, consists in carrying out the approximation on the full Finite Element vector fields using POD modes and Galerkin projection [35]. POD-Galerkin approaches are based on a low-dimensional projection of the PDE equations so that it is accurate in some sense and the physics is included into the equations. However, it is known that the POD-Galerkin method may become unstable for convection-dominated problems, and stabilization/up-winding fixes are required. Moreover, these approaches are intrusive: the computational code must be accessible in order to build the reduced system to solve. In the present work, we rather use a fully non-intrusive approach which consists of growing database of fine solutions with some interpolation process and control of the accuracy. In some sense, it is a set of stable local reduced order models with trust region. The reduction of both space and parameters is performed by a combination of the POD method with the ISAT algorithm [9, 10].

5.1. The ISAT algorithm

The purpose of the ISAT algorithm [9] is to tabulate a function $f(x)$:

$$\begin{aligned} f \quad &: \quad \mathbb{R}^p \longrightarrow \mathbb{R}^m \\ &\qquad \theta \mapsto f(\theta). \end{aligned}$$

where θ and f are respectively input vector and output vector. In the context of this work, the input θ is the design parameter vector and the output is the temperature field in the cabin. Given a query, θ^q, ISAT returns $\tilde{f}(\theta^q)$, an approximation to $f(\theta^q)$. Then we define $\epsilon = \|\tilde{f}(\theta^q) - f(\theta^q)\|$ the approximation error. An essential aspect of ISAT is that the table is built up, not in a pre-processing stage, but in situ (or "on line") as the simulation is being performed. An other important aspect is that ISAT can control the size of the table so that the approximation error is probably less than a given tolerant value noted by ϵ_{tol}. At the beginning, the table is empty. Then the entries are added as needed based on the queries θ^i and on it's output $f(\theta^i)$ computed by the fine simulation. Each entry is considered as a leaf of a binary tree. The ith leaf includes:

- its location θ^i;
- the function value $f^i = f(\theta^i)$;
- a jacobian matrix A^i, which has components;

$$A^i_{kl} = \frac{\partial f^k}{\partial \theta_l}(\theta^i)$$

- The ith region of accuracy (ROA) of the leaf in parameters space.

The matrix A^i is used to construct a local linear approximation. Given a query θ^q, the approximation to $f(\theta)$ based on the ith leaf is defined as:

$$\tilde{f}(\theta^q) = f^i + A^i(\theta^q - \theta^i) \tag{13}$$

DOI: 10.1002/nme

The ROA is defined to be the connected region containing θ^i, in which the error of the linear approximation is less than the specified tolerance ϵ_{tol}. In original ISAT, the ROA is approximated by an ellipsoid, called the ellipsoid of accuracy(EOA) whose center is θ^i. The EOA is initialized conservatively, and it may subsequently be modified (or grown) as additional information about the ROA is generated. Then, there are 3 different scenarios:

- **Retrieve attempt**: For a new point query θ^q, the ISAT algorithm will identify a leaf such that the EOA covers this point. If such a leaf is found, the linear approximation to $f(\theta^q)$ based on that leaf is returned.
- **Grown attempt**: If the first attempt is unsuccessful, then $f(\theta^q)$ is directly evaluated by referent simulation. Some number of leaves that in some sense are close to θ^q are selected for *grown attempt*. Based on each of these selected leaves, the error ϵ in the linear approximation to $f(\theta^q)$ is evaluated, and if it is less than ϵ_{tol} then the leaf's EOA is grown to cover θ^q and $f(\theta^q)$ is returned. The new EOA will be the minimum ellipsoid which covers the old EOA and θ^q (see [36] for more detail).
- **Add**: If the grown attempt is unsuccessful, then the new leaf containing θ^q is added to the binary tree.

In this way, the ISAT is as an efficient storage and retrieval method. The new entry is stored in the table as needed and is indexed by the leaf of a binary tree. A new stored leaf's EOA is distinguished with previous EOAs by a cutting plane. The information of theses cutting planes is stored in the nodes of the binary tree. Thanks to these ones, ISAT finds out rapidly the EOAs that cover or are nearest to the query point in the parameter space. The biggest limitation of ISAT is the requirement of gradient matrix. Hedengren [37] provided a new development in the case where A is unknown using linear regression of gradient matrix based on previous input-output data. Varshney and Armaou [38] used finite differences with common random numbers. However, the accuracy of computing this matrix will not influence the error control, but will likely decrease the efficiency of ISAT. In addition, the ISAT proved its performance in the case low dimension of output (50-100). In the context of CFD, the output may be velocity field or temperature field which have the high dimension (= number of node $> 10^6$). The POD is one of the best method to reduce the dimensionality of CFD fields. For these reasons, this paper proposes a combination of ISAT and POD to build a reduced order model applicable to the design of aircraft air control systems.

5.2. Design of Computer Experiment(DoCE)

The parameter space sampling is an important issue for the accuracy of any meta-model. Commonly used DoCE procedure include Latin Hypercube Sampling (LHS), U-designs [39] and Lattice Design [40]. In this work, we used LHS method to build our DoCEs. Let N_{init} be the number of design sites in the parameter space chosen according to a LHS design procedure. After computing the exact solutions (e.g. the temperature fields) for these design sites by a FE code, an initial snapshot set $\mathcal{S}^{N_{init}}$ is formed as follows:

$$\mathcal{S}^{N_{init}} = \left\{T^i,\ i = 1, \ldots, N_{init}\right\}. \tag{14}$$

For each snapshot of $\mathcal{S}^{N_{init}}$, defined by a solution T^i corresponding to the vector of design parameters θ^i ($T^i = T(\theta^i)$), a lifting function T^{lift,θ^i} is computed as the solution of the following problem:

$$\triangle T^{lift,\theta^i} = 0 \quad \text{in } \Omega, \tag{15}$$

$$T^{lift,\theta^i} = T_{in} \text{ on } \Gamma_{in},\ \frac{\partial T^{lift,\theta^i}}{\partial n} = 0 \text{ on } \Gamma_{out},\ \kappa \frac{\partial T^{lift,\theta^i}}{\partial n} = \Phi(T^{lift,\theta^i} - T_{ext}) \text{ on } \Gamma_w \tag{16}$$

Note that the solution depends linearly on the Dirichlet boundary condition T_{in}. To reduce the computational cost, this equation is solved once by a FE method for the boundary condition $T_{in} = 1$. The corresponding solution, called $T^{lift,1}$ is stored. Then solution of (15,16) for an arbitrary T_{in} is simply: $T^{lift,\theta^i} = T_{in}.T^{lift,1}$.

DOI: 10.1002/nme

5.3. *Local form of the POD-ISAT ROM*

Assume that we are at the addition step, so the current query parameter θ^i becomes a new entry for the table, say the ith entry. The corresponding solution T^i (e.g. temperature field) is computed by the FE model. Then a new local reduced order model is built up at θ^i. Firstly, we need to compute the good POD modes, then build up a local approach for the neighbour of θ^i. The local POD modes are computed by a subset of samplings consisting in N_{local} nearest (in the sense of the euclidean norm in the parameter space) points of θ^i:

$$\mathcal{S}_{(i)}^{N_{local}} = \left\{ (T^j - T_{(i)}^{lift,\theta^j}),\ j = 1, \ldots, N_{local} \right\}, \tag{17}$$

with $T_{(i)}^{lift,\theta^j} = T^{lift,\theta^j} + (T^i - T^{lift,\theta^i})$ the concentrated lifting function.
The truncation order K^i is chosen so that the energy captured by the K^i first modes is higher than a confidence threshold. In other word, the error of projection is expected to be less than a tolerance value. However, for the sake of clarity, we will fix $K^i = K$ for all local ROMs. The local form of ISAT-POD reads as follows:

$$\tilde{T}_{(i)}^{\theta}(x) = T_{(i)}^{lift,\theta}(x) + \sum_{k=1}^{K} a_{(i)}^k(\theta)\, \mathbf{\Psi}_{(i)}^k(x), \tag{18}$$

where the local POD coefficients $a_{(i)}^k$ depends on the design parameters θ and θ^i.

5.3.1. Local POD coefficients Generally, these local POD coefficients $a_{(i)}^k$ are unknown at θ. Note that we can compute these ones at the N_{local} sampling points θ^j as the coefficients of POD projection:

$$a_{(i)}^k(\theta^j) = \left(T^j(x) - T_{(i)}^{lift,\theta^j}(x), \mathbf{\Psi}_{(i)}^k(x) \right); k = 1, \ldots, K; j = 1, \ldots, N_{local}. \tag{19}$$

Using (19), the coefficients $a_{(i)}^k(\theta)$ can be interpolated or approximated by standard robust methods (Moving Least Square (MLS) [41, 42], artificial neural networks (ANN) [43], radial basis functions (RBF) [34] or Kriging approaches [44]). In this paper we used the kriging technique provided by the DACE Toolbox [†] to approximate the K POD coefficients.

$$\begin{aligned} \tilde{a}_{(i)}^k \quad &: \quad \mathbb{R}^p \longrightarrow \mathbb{R} \\ &\theta \mapsto \tilde{a}_{(i)}^k(\theta), \quad k = 1, ..., K. \end{aligned} \tag{20}$$

Alternatively, the coefficients $a_{(i)}^k(\theta)$ can also be determined by minimizing the $\mathcal{L}^2$ norm of the residual presented in the equation (7):

$$(a_{(i)}^1, \ldots, a_{(i)}^K)(\theta) = \arg \min_{(a_{(i)}^1, \ldots, a_{(i)}^K)} \frac{1}{2} \left\| R\left(T_{(i)}^{lift,\theta}(x) + \sum_{k=1}^{K} a_{(i)}^k(\theta)\, \mathbf{\Psi}_{(i)}^k(x) \right) \right\|_{\mathcal{L}^2}^2. \tag{21}$$

The optimization problem (21) can be solved by means of standard search algorithms in low dimension. We assume that, the FE code or FV code allows to compute the residual of any solution. The cost of computing the residual is cheaper than the computation of one solution. We used a standard optimization algorithm to make the implementation easy and maintain the non-intrusive feature. The initial guess for $a_{(i)}^k$ is important as it conditions the efficiency of the optimization. One can choose the initial guess as follows: $a_{(i)}^k(\theta^i) = 0$, $k \in [1, \ldots, K]$. Another way is to initialize with the interpolated values of the coefficients using (20).

[†] http://www2.imm.dtu.dk/~hbn/dace/

DOI: 10.1002/nme

5.3.2. Trust region (TR) The local representation (18) is valid in a trust region denoted by $\mathcal{E}(i)$ defined as a ball or an ellipsoid centred in θ^i. Once this trust region is determined, a supplementary random sampling $(\theta^j)_{j=1,\dots,N_{sup}} \in \mathcal{E}(i)$ within the TR is generated and the local POD coefficients $a^k_{(i)}(\theta^j)$, $k \in [1,\dots,K]$, $j \in [1,\dots,N_{sup}]$ are computed by (21). Then, using these coefficients, a high-dimensional interpolation (kriging for example) of $a^k_{(i)}(\theta)$ is built one more time. Thus, the local ROM attached to the point θ^i is completely defined by the formula (18), its trust region and the POD coefficient interpolation model $\tilde{a}^k_{(i)}(\theta)$. Then this new record can be added to the database. The adaptive enrichment process is aimed at covering the whole design domain. Below we provide the whole details of the algorithm, especially the construction of the trust region.

5.4. Trust region building

Assume that a new database record is currently constructed. We need to characterize a Trust Region around θ^i. Assuming that the POD coefficients are continuous in the parameter space, there is a region $\mathcal{E}(i)$ such that the residual field satisfies

$$\forall \theta \in \mathcal{E}(i) \quad \left\| R(\tilde{T}_{(i)}(\theta)) \right\|_{\mathcal{L}^2} \leq \varepsilon_{tol} . \left\| R_0 \right\|,$$

where $\varepsilon_{tol} \ll 1$, and $\|R_0\|$ is a reference residual. For computational conveniences, the trust region $\mathcal{E}(i)$ is searched as an ellipsoid, as initially proposed by Pope [9]. The so-called ellipsoid of accuracy (EOA) in $\mathbb{R}^p$ is uniquely defined by $\frac{p^2+p}{2}$ variables. The TR is determined by finding out $M > \frac{p^2+p}{2}$ different θ^* in the vicinity of θ^i such that $\|R(\theta^*)\|_{\mathcal{L}^2} = \varepsilon_{tol}$. The sample points θ^* are searched in the form $\theta^* = \theta^i + \alpha^* h$, with $\alpha^* \in \mathbb{R}$ and $h \in \mathbb{R}^p$ is a fixed unit vector. By randomly choosing M different vectors h, M points θ^*_h are computed in parallel as the M minimization problems are independent (see Figure 2). So this algorithm is particularly suited for today's many-core computer architectures. Practically we have used the Matlab Ellipsoidal Toolbox [‡]. This toolbox allows to build an ellipsoid which forms the contour of the boundary points θ^*_h. This initial EOA does not strictly guarantee the residuals to be less than the given threshold with the ellipsoid. However, this initial EOA is used to generate sampling points inside to build the kriging interpolation model $\tilde{a}^k_{(i)}$. Thanks to these samples, we adapt the EOA boundary so that the sampling points residuals are less than the given threshold. The size of the EOA obviously depends on the choice of tolerance threshold ε_{tol}.

5.5. Summary of POD-ISAT algorithm

The POD-ISAT algorithm consists of 2 stages. The first one is called the off-line preliminary stage and the second one is the on-line building stage. Initially, POD-ISAT algorithm needs a preliminary sampling $\mathcal{S}^{N_{init}} = \left\{T^i,\ i = 1,\dots,N_{init}\right\}$. The sampling parameters are generated by a space-filling sampling method (for example Latin Hypercube Sampling, LHS) and the corresponding (fine) solutions are computed by Finite Elements or Finite Volumes method. In practice, these independent computations can be done in parallel. Thanks to this initial sampling, the corresponding local ROMs for each θ^j in $\mathcal{S}^{N_{init}}$ are built if needed. Let us consider now a next query point of initial sampling. If it belongs to the trust region of an existing record, we do not need to build the local ROM at this point, but we can save it in the database for the purpose of local POD construction (see algorithm 1). In the end of this stage, the database consists of $n_{record} \leq N_{init}$ local ROMs. In the next stage, the sample within its local ROM will be built up adaptively and added in the database (see algorithm 2). For the new query point θ^q, the POD-ISAT algorithm looks for a trust region which covers this entry. If the research is successful, then we have a local ROM candidate and the approximate solution will be returned instantaneously. Otherwise, a new record will be added in the database. Progressively, the design parameter space will be filled up by all the overlapping trust regions.

[‡] http://www.mathworks.com/matlabcentral/fileexchange/21936-ellipsoidal-toolbox-et

DOI: 10.1002/nme

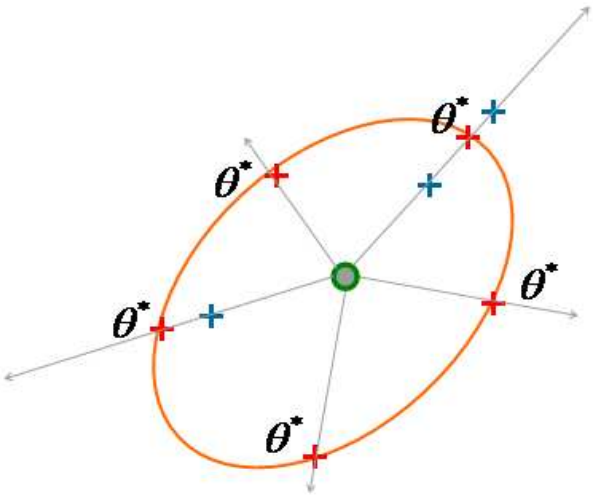

Figure 2. Trust region building (for each random direction, one finds out a point θ^* such that $\|R\|^2 - \epsilon_{tol} \leq 0$, this point will be used to define the boundary of EOA)

Data: Preliminary sampling of design parameter space using a DoCE procedure
Result: Preliminary adaptive Database

Compute the Finite Element solution for the preliminary sampling:
$\mathcal{S}^{N_{init}} = \left\{T^j = T(\theta^j),\ j = 1, \ldots, N_{init}\right\}$
for $i = 1$ **to** N_{init} **do**
  if $n_{records} = 0$ **then**
    Build the first local ROM at θ^i
  else
    Look for EOA which covers θ^i by the retrieve stage of ISAT.
    if *The retrieve stage is successful* **then**
      Define scenario='retrieve';
      We stock only (T^{θ^i}, θ^i) in the Database
    else
      Define scenario='addition';
      Build the new local ROM together with EOA at θ^i.
      Add this new information record to the Database.
    end
  end
end

Algorithm 1: Preliminary stage of POD-ISAT

6. NUMERICAL RESULTS

The POD-ISAT method was tested on the use case described in section 3.

6.1. Aircraft air control system with two parameters

In this case, two design parameters are considered, the first is the temperature of air injected by the main ventilation T_{in} and the second is the fuselage thermal conductivity κ_f. These two parameters are supposed to vary within reasonable admissible intervals: $T_{in} = [T_{in}^{min} = 21, \cdots, T_{in}^{max} = 28](^\circ\mathrm{C})$; $\kappa_f = [\kappa_f^{min} = 10^{-4}, \cdots, \kappa_f^{max} = 10^{-3}](W \cdot m^{-1} \cdot K^{-1})$. The normalized parameters

DOI: 10.1002/nme

Input: New query parameter θ^q
Output: Approximate solution $\tilde{T}^{\theta^q}$

Look for EOA containing θ^i which covers θ^q by the retrieve stage of ISAT.
if *The retrieve stage is successful* **then**
  Define scenario='retrieve';
  The solution is approached by: $\tilde{T}^{\theta^q}_{(i)}(x) = T^{lift,\theta^q}_{(i)}(x) + \sum_{k=1}^{K} a^k_{(i)}(\theta^q)\, \mathbf{\Psi}^k_{(i)}(x)$.
else
  Define scenario='addition';
  Call the fine simulation for θ^q.
  Build the new local ROM together with EOA at θ^q.
  Add this new information record to the Database.
  The fine solution is returned: $\tilde{T}^{\theta^q}(x) = T^{\theta^q}(x)$
end

Algorithm 2: Online building stage of POD-ISAT

$\theta = [\theta_1 \quad \theta_2]^t$ are defined as follows:

$$\theta_1 = \frac{T_{in} - \frac{1}{2}(T_{in}^{min} + T_{in}^{max})}{\frac{1}{2}(T_{in}^{max} - T_{in}^{min})},$$

$$\theta_2 = \frac{\kappa_f - \frac{1}{2}(\kappa_f^{min} + \kappa_f^{max})}{\frac{1}{2}(\kappa_f^{max} - \kappa_f^{min})},$$

The air is initially at rest and at uniform temperature in the cabin ($T_0 = 20°\mathrm{C}$). The hot air is injected at the fuselage's bottom and at the top of the cabin. After 220 time iterations, the flow is almost stationary. We give for example four solutions (temperature fields) for four parameter vectors, chosen randomly in the admissible space (see the figure 3).

6.1.1. POD ROM sensitivity In the view of evaluating the POD ROM sensitivity, a "small" DoCE of nine reference solutions was computed. The first 4 modes are presented in figure 4. The formula (18) was used to build the POD ROM using kriging method to interpolate the POD coefficients. Then, the parameter T_{in} was fixed and the parameter κ_f was varied. To assess the sensitivity of the local ROM model with respect to the number of POD modes, we tested three different values of n_{POD}. For each value of the integer n_{POD}, the residual (7) of the POD ROM was minimized to obtain the POD coefficients (21) for 24 points uniformly distributed over the range of variation of the design parameter κ_f. The results are shown in figure 5, where the optimal residual is normalized by a reference residual $R_0 = 10^{-5}$. As expected, it is observed that the relative value of optimal residual ($\|R^{opt}\|/\|R_0\|$) is smaller when n_{POD} is bigger. If we take into account more POD modes, we obtain a more accurate approach. For this particular case, we found that we can only consider 4 POD modes to build a reasonably accurate reduced model. Furthermore, we assume that if the relative residual is less than 2, the corresponding POD ROM can be considered as accurate. For areas around $\theta_2 = -1$ or around $\theta_2 = -0.5$, the POD ROM is not reliable (see figure 5). It is probably due to a lack of "good" information, i.e. a lack of sample snapshots at these areas. However, in the region of $\theta_2 = 0, \cdots, 1$, the reduced model is accurate. Therefore, there are areas in the design parameters space where the POD ROM is accurate and others where it is not. A way to improve the accuracy of the POD ROM model is to add snapshots in the areas where the model is not accurate. The POD-ISAT model adds new snapshots in these regions and builds up trust regions to control the model's accuracy, it is then expected to be more reliable and accurate.

6.1.2. POD-ISAT ROM building To start building the POD-ISAT database, we need a preliminary snapshot set. For that we applied the algorithm 1-2. The choice of the open parameters of POD-ISAT

DOI: 10.1002/nme

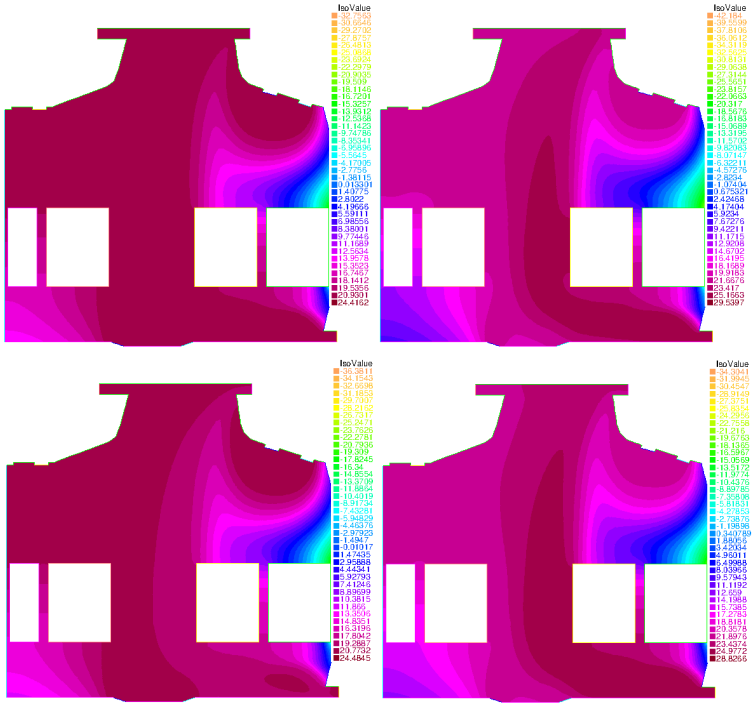

Figure 3. Reference Finite Element temperature solutions for four random parameter samples.

Table I. Properties of POD-ISAT reduced model

N_{init}	10	Initial DoCE Size
ε^2_{tol}	2	Threshold of relative residual
N_{local}	9	Number of nearest neighbours used to build local POD
K	4	Number of POD modes used
p	2	Number of parameters

ROM is summarized on the table I. Next, we give more details on the different POD-ISAT stages.
Preliminary stage: At the beginning of this stage 10 reference FE solutions are computed relying on LHS sampling. At the end of this stage, $n_{records} = 3$, i.e there are 3 local ROMs which are built for three different parameter points. The other sampling points belong to these ROM's EOA. So we do not need to build local ROM at these points. However we need to save their computed exact solutions for use in the construction of local POD bases later.
On-line building stage: A number of 190 randomly generated query points are used by the algorithm 2. When POD-ISAT algorithm finishes, we have $n_{records} = 9$, i.e there are 9 local reduced models in the database. The final $EOAs$ are showed in the normalized parameter space ($\theta \in [-1; 1]^2$) (see figure 6). The $EOAs$ cover almost the entire design parameter space. It is worth noticing that the POD-ISAT algorithm has examined 200 query points in total (preliminary stage and on-line stage). These points are used to check the accuracy of the POD-ISAT approach. We computed all the fine FE solutions at these query points. Then, the POD-ISAT ROM solutions are

DOI: 10.1002/nme

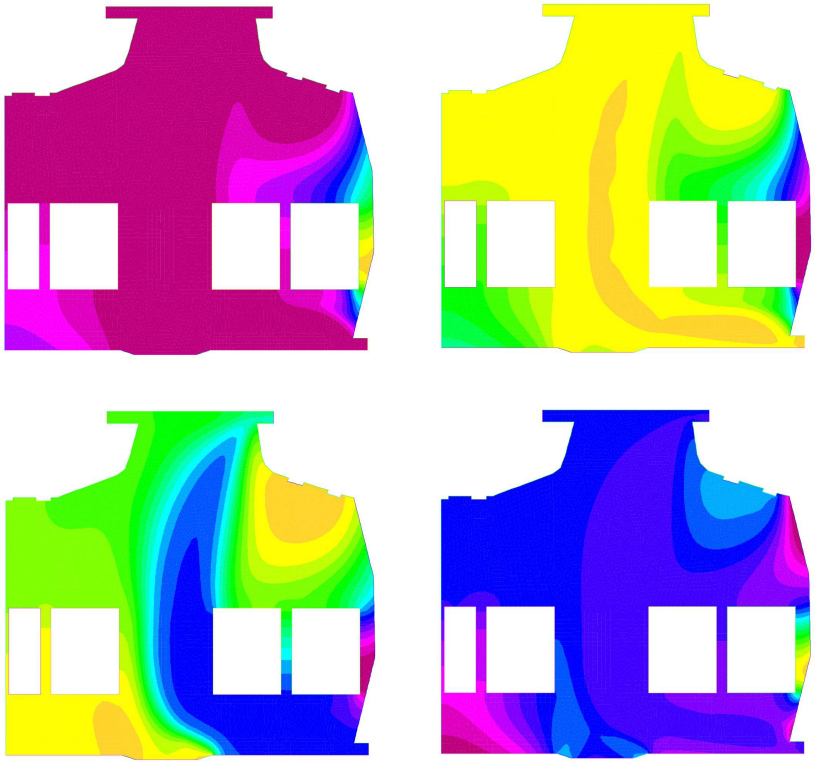

Figure 4. Isocontours of the four first POD eigenmodes: $\mathbf{\Psi}^1$(top-left), $\mathbf{\Psi}^2$ (top-right), $\mathbf{\Psi}^3$ (bottom-left), $\mathbf{\Psi}^4$ (bottom-right).

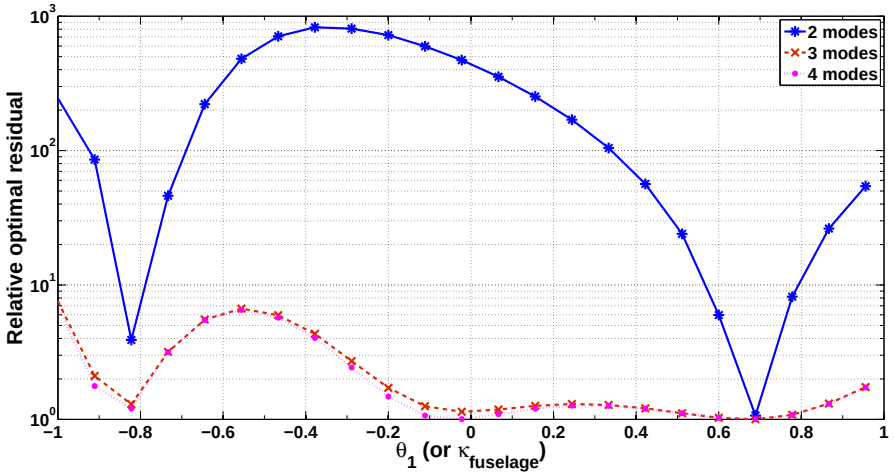

Figure 5. Relative optimal residual values according to the value of $\kappa_{fuselage}$ and the number of modes taken in account n_{POD}

compared with the corresponding FE solutions using the following error criterion (relative error):

$$\text{relative error} = \frac{\|\tilde{\boldsymbol{u}}(\theta) - \boldsymbol{u}(\theta)\|_{\mathcal{L}^2}}{\|\boldsymbol{u}(\theta)\|_{\mathcal{L}^2}}. \tag{22}$$

DOI: 10.1002/nme

The distribution of the relative error values over the design parameter space is shown in figure 7, where one can find that the maximum relative error is 1.2×10^{-3}. This maximal error occurs close to a boundary of the design space parameter domain in the area of low inlet temperatures T_{in} and high fuselage conductivities κ_f. One explanation is that for high fuselage conductivities, the solution can become unsteady and the changes of the solution in this area (high κ_f and low T_{in}) may become difficult to approach with a steady assumption.

Using the same test case and the same database size, we built a non intrusive POD ROM using the

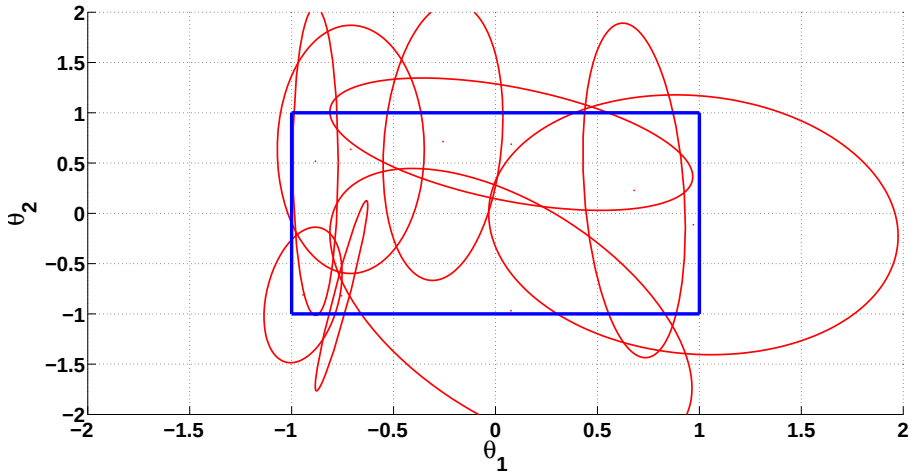

Figure 6. Representation of the EOAs covering the design space parameter $[-1;1]^2$ (rectangle)

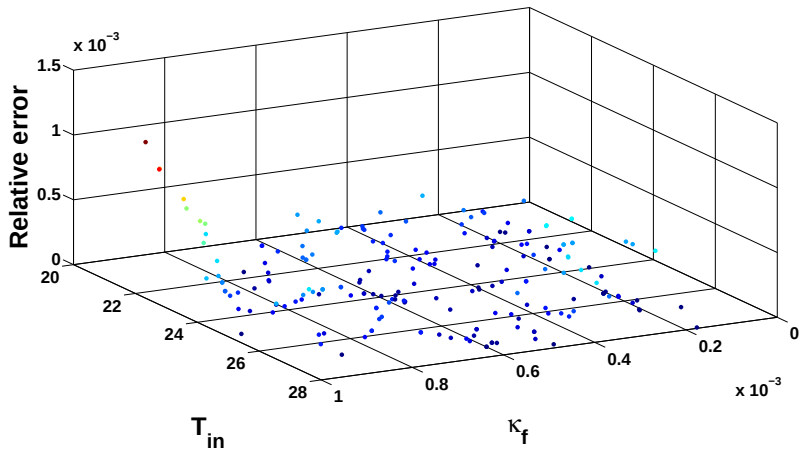

Figure 7. Relative errors for 200 queries computed by POD-ISAT ROM in design parameter space with 2 parameters

formula (18). In the preliminary step of the POD-ISAT algorithm, described in 1-2, 10 reference solutions are computed and only 3 of them are added to the database to generate the initial $EOAs$. Then at the end of the second stage (on-line stage), 6 points are added to the database to cover the whole design parameter space with 9 $EOAs$. To compute the POD modes, we formed a snapshot matrix of 16 points, 10 of them are the same as the 10 initial reference FE solutions quoted above and the remaining 6 others are generated by a LHS procedure. The POD coefficients are computed using a standard kriging method.

Then, the POD ROM was evaluated on the same 200 query points as outlined above and the relative

DOI: 10.1002/nme

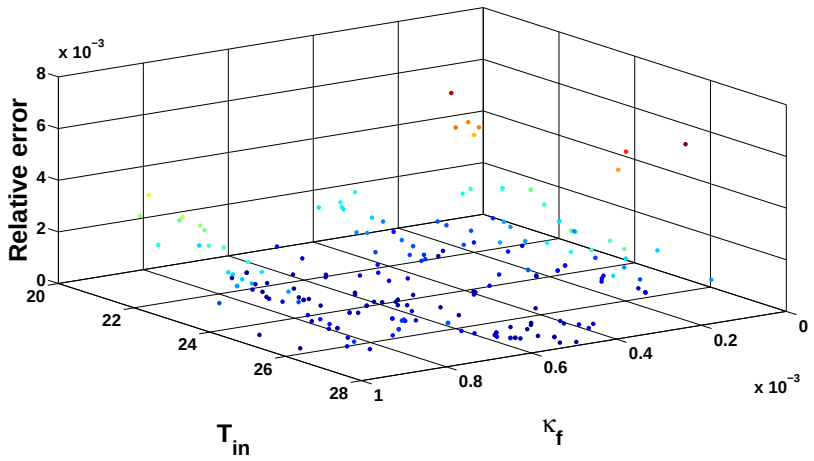

Figure 8. Relative errors for 200 queries computed by POD ROM in design parameter space with 2 parameters

error with FE solutions was computed. The distribution of the POD ROM relative error over the design parameter space is shown on figure 8, where one can see that, like for POD-ISAT (see figure 7), the maximal error occurs close to a boundary of the design space parameter domain in the area of low inlet temperatures T_{in} and high fuselage conductivities κ_f. But, unlike POD-ISAT, the POD ROM is inaccurate also in the area of low inlet temperatures T_{in} and low fuselage conductivities κ_f. The maximal relative error and the mean relative error have been computed over 200 queries as can be seen on figure 9. It can be noticed that the POD-ISAT method is far more efficient than the standard POD method.

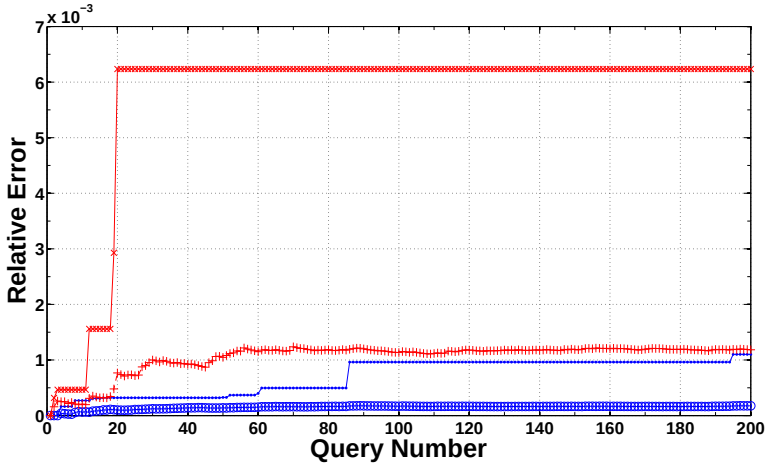

Figure 9. Maximal relative errors for POD ($\times$) and POD-ISAT ($\bullet$) and Mean relative errors for POD ($+$) and POD-ISAT ($\bigcirc$) for 2 parameters

6.2. Aircraft air control system with four parameters

To show the ability of the method to deal with high dimensional cases, we added in this test case 2 more design parameters (see figure 10). The first one is the inlet temperature $T_{in,a}$ at the aisle Γ^1_{in} and the second one is the private inlet temperature $T_{in,p}$ above the passenger head Γ^2_{in}. These 2 parameters vary from $T^{min}_{in,a} = T^{min}_{in,p} = 21°\mathrm{C}$ to $T^{max}_{in,a} = T^{max}_{in,p} = 28°\mathrm{C}$. The dimensionless design

DOI: 10.1002/nme

parameter vector $\theta = [\theta_1 \quad \theta_2 \quad \theta_3 \quad \theta_4]^t$ is defined as follows:

$$\theta_1 = \frac{T_{in} - \frac{1}{2}(T_{in}^{min} + T_{in}^{max})}{\frac{1}{2}(T_{in}^{max} - T_{in}^{min})},$$

$$\theta_2 = \frac{\kappa_f - \frac{1}{2}(\kappa_f^{min} + \kappa_f^{max})}{\frac{1}{2}(\kappa_f^{max} - \kappa_f^{min})},$$

$$\theta_3 = \frac{T_{in,a} - \frac{1}{2}(T_{in,a}^{min} + T_{in,a}^{max})}{\frac{1}{2}(T_{in,a}^{max} - T_{in,a}^{min})},$$

$$\theta_4 = \frac{T_{in,p} - \frac{1}{2}(T_{in,p}^{min} + T_{in,p}^{max})}{\frac{1}{2}(T_{in,p}^{max} - T_{in,p}^{min})},$$

We generated $N_{init} = 20$ preliminary samples still using LHS space-filling technique. At the beginning, the algorithm 1 built up the first ROMs based on the preliminary samples. At the end of this stage $n_{records} = 9$. Then 400 queries generated by LHS are called by the second stage. At the end we have $n_{records} = 28$. The relative error computed for the 420 queries are given in figure 11.

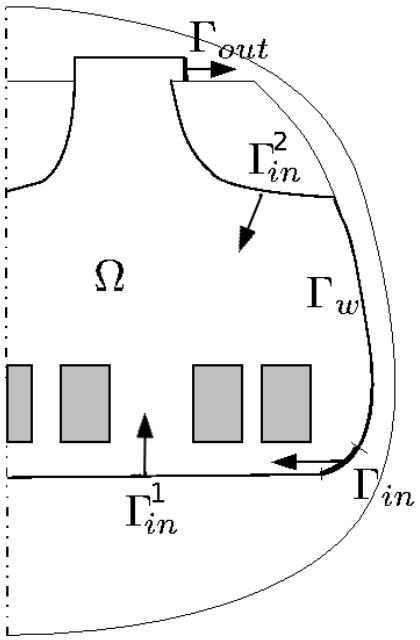

Figure 10. Two added design parameters are inlet temperature at the aisle and above the head of passenger

The maximal relative error and the mean relative error have been computed for 420 queries as can be seen on figure 12. It can be noticed that the POD-ISAT method is more efficient than the standard POD method.

6.3. CPU costs evaluation

The significant CPU costs are analysed in the following. The simulation is performed on an Intel Core I7 Computer. The FE model is implemented on `FreeFem++3.10` [§] and the POD-ISAT algorithm is implemented on `Matlab` [¶]. The computation time consists of on-line time and outline

[§]http://www.freefem.org/ff++/
[¶]http://www.mathworks.fr/products/matlab/

DOI: 10.1002/nme

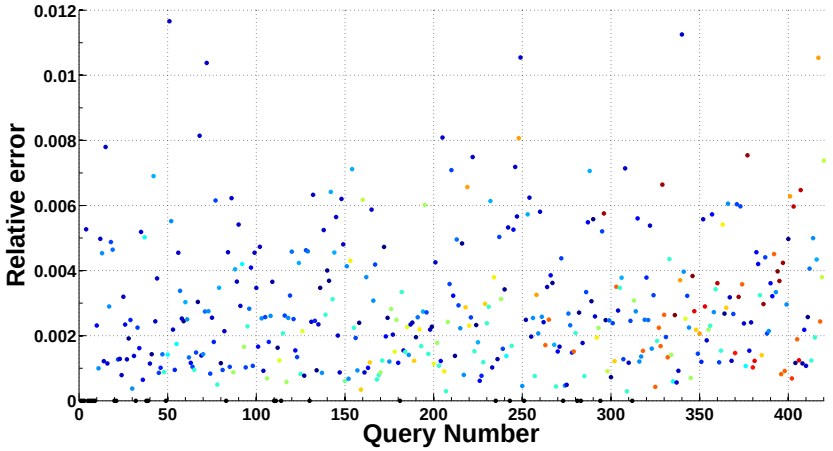

Figure 11. Relative errors for 420 queries computed by POD-ISAT for 4 parameters

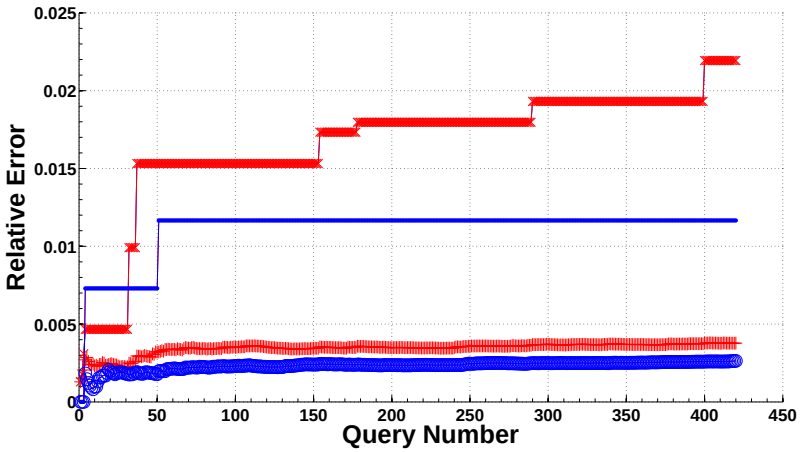

Figure 12. Maximal relative errors for POD ($\times$) and POD-ISAT ($\bullet$) and Mean relative errors for POD ($+$) and POD-ISAT ($\bigcirc$) for 4 parameters

time. The POD-ISAT algorithm involves different elementary operations that induce associated CPU costs. The first one is the CPU cost associated with the fine evaluation of one single FE solution. The second one, called "retrieve cost", is the time spent to search the database for the right EOA plus the time to evaluate the POD-ISAT ROM (18). The third one is the time spent to build an EOA. The last one is the time spent to build a kriging model. These costs are outlined in Table II. For the use case with two parameters 6.1, it took 7 hours of computation to build the database by evaluating the 200 query points and building the EOAs. For the use case with four parameters 6.2, it took 20 hours of computation to build up the database through evaluating 420 query points. Thus, building the database can be computationally intensive but it provides the coverage of the whole design parameter space with an accurate representation of the solutions compared to standard POD. The speed-up, defined as the ratio of the time to evaluate a solution with the FE code by the time needed to compute a solution with the POD-ISAT ROM once the database has been built up, is $1000/0.89 \sim 10^3$, which shows the computational efficiency of the POD-ISAT method.

DOI: 10.1002/nme

	Online	Outline
EOA Building		1200 sec
Kriging model		300 sec
FE computation of $u(x, \theta)$		1000 sec
Retrieve	0.89 sec	

Table II. CPU costs

7. CONCLUDING REMARKS

In this paper, a general PDE non-intrusive adaptive reduced modelling strategy has been presented. It combines both Proper Orthogonal Decomposition (POD) for strong dimensionality reduction, and In Situ Adaptive Tabulation (ISAT) for fast evaluation of a time-consuming function by means of a database model. The so called POD-ISAT algorithm has been tested and evaluated on a design problem design of aircraft cabin air control system (ACS). The numerical results show that the ROM provides both high efficiency and accuracy in its on-line use. Of course it requires time-consuming evaluations of fine Finite Elements solutions during the learning stage and enrichment process. The Trust Region (TR) strategy allows us to control the accuracy of the model. However, it has been observed that the EOA can be inaccurately defined and as already pointed out in papers related to ISAT (see [10]). This problem can be tackled by adding a so-called 'Ellipsoid Of Inaccuracy' (EOI) to control the inaccuracy of the EOA estimator. Furthermore, the ε_{tol} controls the error on the residual and not on the solution itself which is not convenient, which points out the need to consider more appropriate easy-to-compute a-posteriori error estimators.

ACKNOWLEDGEMENT

This work is supported by the industrial platform 'Complex System Design Lab' CSDL, Pôle de Compétitivité System@tic, Paris Région Ile-de-France, 2009-2012. We thank Dr. John Hedengren for helping us with ISAT algorithm on Matlab.

REFERENCES

1. G Berkooz, P Holmes, and JL Lumley. The proper orthogonal decomposition in the analysis of turbulent flows. *Annual review of fluid mechanics*, 25:539–575, 1993.
2. Kevin Carlberg and Charbel Farhat. A low-cost, goal-oriented compact proper orthogonal decomposition basis for model reduction of static systems. *International Journal for Numerical Methods in Engineering*, 86(3):381–402, 2011.
3. T. Bui-Thanh, K. Willcox, O. Ghattas, and B. van Bloemen Waanders. Goal-oriented, model-constrained optimization for reduction of large-scale systems. *J. Comput. Phys.*, 224(2):880–896, June 2007.
4. Yvon Maday and Einar M. Ronquist. A reduced-basis element method. *Comptes Rendus Mathématique*, 335(2):195 – 200, 2002.
5. G. Rozza, D. Huynh, and A. Patera. Reduced basis approximation and a posteriori error estimation for affinely parametrized elliptic coercive partial differential equations. *Archives of Computational Methods in Engineering*, 15:229–275, 2007. 10.1007/s11831-008-9019-9.
6. Ladevèze Pierre. *Nonlinear Computational Structural Mechanics. New Approaches and Non-Incremental Methods of Calculation*. Mech. Eng. Series. Springer-verlag, 2009.
7. A. Ammar, B. Mokdad, F. Chinesta, and R. Keunings. A new family of solvers for some classes of multidimensional partial differential equations encountered in kinetic theory modeling of complex fluids. *Journal of Non-Newtonian Fluid Mechanics*, 139(3):153 – 176, 2006.
8. D. Ryckelynck. A priori hyperreduction method: an adaptive approach. *Journal of Computational Physics*, 202(1):346 – 366, 2005.
9. S.B. Pope. Computationally efficient implementation of combustion chemistry using in situ adaptive tabulation. *Combustion Theory and Modelling*, 1(1):41–63, 1997.
10. Liuyan Lu and Stephen B. Pope. An improved algorithm for in situ adaptive tabulation. *Journal of Computational Physics*, 228(2):361 – 386, 2009.

DOI: 10.1002/nme

11. Board on Environmental Studies Committee on Air Quality in Passenger Cabins of Commercial Aircraft, Toxicology Division on Earth, and National Research Council Life Studies. *THE AIRLINER CABIN ENVIRONMENT AND THE HEALTH OF PASSENGERS AND CREW*. NATIONAL ACADEMY PRESS, 2002.
12. Rogers DJ. Tatem AJ, Hay SI. Global traffic and disease vector dispersal. *Proc Natl Acad Sci U S A*, (103(16):6242e7), 2006.
13. Pavia AT. Germs on a plane: aircraft, international travel, and the global spread of disease. *J Infect Dis*, (195(1):621e2), 2007.
14. Cheung T Tang A Fisk T Ooi S et al. Olsen S, Chang H. Transmission of thesevere acute respiratory syndrome on aircraft. *New England J Med*, (349(25):2416e22), 2003.
15. T Zhang and Q Chen. Novel air distribution systems for commercial aircraft cabins. *Building and Environment*, 42(4):1675–1684, 2007.
16. Tengfei (Tim) Zhang, Shi Yin, and Shugang Wang. An under-aisle air distribution system facilitating humidification of commercial aircraft cabins. *Building and Environment*, 45(4):907 – 915, 2010.
17. J. — Lammen W.F. Vankan, W.J. — Kos. Approximation models for multi-disciplinary system design - application in a design study of power optimised aircraft. Technical report, National Aerospace Laboratory NLR, Amsterdam, The Netherlands, 2003.
18. P.O. Fanger. *Thermal comfort - Analysis and applications in environmental engineering*. PhD thesis, TU Denmark, 1970.
19. Sjoerd S. Burgers Henry Dol Stefan P. Spekreijse Johan C. Kok, Jaap van Muijden. Enhancement of aircraft cabin comfort studies by coupling of models for human thermoregulation, internal radiation, and turbulent flows. ECCOMAS CFD 2006, 2006.
20. Shinichi Tanabe, Kozo Kobayashi, Junta Nakano, Yoshiichi Ozeki, and Masaaki Konishi. Evaluation of thermal comfort using combined multi-node thermoregulation (65mn) and radiation models and computational fluid dynamics (cfd). *Energy and Buildings*, 34(6):637 – 646, 2002. Special Issue on Thermal Comfort Standards.
21. Wei Liu, Sagnik Mazumdar, Zhao Zhang, Stephane B. Poussou, Junjie Liu, Chao-Hsin Lin, and Qingyan Chen. State-of-the-art methods for studying air distributions in commercial airliner cabins. *Building and Environment*, 47(0):5 – 12, 2012. International Workshop on Ventilation, Comfort, and Health in Transport Vehicles.
22. F. De Vuyst. *Multidisciplinary Design Optimization in Computational Mechanics*, chapter PDE Metamodeling using Principal Component Analysis. Wiley ISTE, April 2010.
23. Kunisch, Karl and Volkwein, Stefan. Optimal snapshot location for computing pod basis functions. *ESAIM: M2AN*, 44(3):509–529, 2010.
24. K. Veroy and A. T. Patera. Certified real-time solution of the parametrized steady incompressible Navier-Stokes equations: rigorous reduced-basis a posteriori error bounds. *International Journal for Numerical Methods in Fluids*, 47(8-9):773–788, 2005.
25. Gianluigi Rozza and Karen Veroy. On the stability of the reduced basis method for Stokes equations in parametrized domains. *CMAME*, 196(7):1244 – 1260, 2007.
26. Simone Deparis. Reduced basis error bound computation of parameter-dependent Navier-Stokes equations by the natural norm approach. *SIAM J. Num. A.*, 46(4):2039–2067, 2008.
27. A. Dumon, C. Allery, and A. Ammar. Proper general decomposition (pgd) for the resolution of Navier-Stokes equations. *Journal of Computational Physics*, 230(4):1387 – 1407, 2011.
28. F. Chinesta, A. Ammar, A. Leygue, and R. Keunings. An overview of the proper generalized decomposition with applications in computational rheology. *Journal of Non-Newtonian Fluid Mechanics*, In Press, Corrected Proof:–, 2011.
29. G. Bonithon, P. Joyot, F. Chinesta, and P. Villon. Non-incremental boundary element discretization of parabolic models based on the use of the proper generalized decompositions. *Engineering Analysis with Boundary Elements*, 35(1):2 – 17, 2011.
30. A. Leygue and E. Verron. A first step towards the use of proper general decomposition method for structural optimization. *ACME*, 17:465–472, 2010. 10.1007/s11831-010-9052-3.
31. M. Beringhier, M. Gueguen, and J. Grandidier. Solution of strongly coupled multiphysics problems using space-time separated representations. application to thermoviscoelasticity. *Arch. of Comp. Methods in Engineering*, 17:393–401, 2010. 10.1007/s11831-010-9050-5.
32. Anthony Nouy. A priori model reduction through proper generalized decomposition for solving time-dependent partial differential equations. *Computer Methods in Applied Mechanics and Engineering*, 199(23-24):1603 – 1626, 2010.
33. P.B Nair, editor. *Physics-based surrogate modeling of parameterized PDEs for optimization and uncertainty analysis*, volume (AIAA-2002-1586). In, Proceedings of 43rd AIAA/ASME/ASCE/AHS/ASC Structures, Structural Dynamics, and Materials Conference. 43rd AIAA/ASME/ASCE/AHS/ASC Structures, Structural Dynamics, and Materials Conference , AIAA,, 2002.
34. C. Audouze, F. De Vuyst, and P. B. Nair. Reduced-order modeling of parameterized pdes using time-space-parameter PCA. *IJNME*, 80(8):1025–1057, 2009.
35. K. Kunisch and S. Volkwein. Galerkin proper orthogonal decomposition methods for a general equation in fluid dynamics. *SIAM J. on Numerical Analysis*, 40(2):492–515, 2002.
36. S.B. Pope. Algorithms for ellipsoids. Technical report, Cornell University FDA, 2008.
37. John D. Hedengren and Thomas F. Edgar. Approximate nonlinear model predictive control with in situ adaptive tabulation. *Computers & Chemical Engineering*, 32(4-5):706 – 714, 2008. Festschrift devoted to Rex Reklaitis on his 65th Birthday.
38. A. Varshney and A. Armaou. *Model Reduction and Coarse-Graining Approaches for Multiscale Phenomena*, chapter An Efficient Optimization Approach for Computationally Expensive Timesteppers using Tabulation, pages pages 513–533. Springer-Verlag, Berlin, 2006.
39. B. Tang. Orthogonal array-based latin hypercubes. *J. Am. St. Asso.*, (88):13921397, 1993.

40. P. Winker K.T. Fang, D.K.J. Lin and Y. Zhang. Uniform previous termdesignnext term: theory and application. *Technometrics*, (42):237248, 2000.
41. P. Lancaster and K. Salkauskas. Surfaces Generated by Moving Least Squares Methods. *Mathematics of Computation*, 37(155):141–158, 1981.
42. Piotr Breitkopf, Hakim Naceur, Alain Rassineux, and Pierre Villon. Moving least squares response surface approximation: Formulation and metal forming applications. *Computers & Structures*, 83(17-18):1411 – 1428, 2005. Advances in Meshfree Methods.
43. Dreyfus Gérard. *Neural networks: methodology and applications*. Editions Eyrolles, 2005.
44. Noel Cressie. The origins of kriging. *Mathematical Geology*, 22:239–252, 1990. 10.1007/BF00889887.

DOI: 10.1002/nme